Communications

A (μ-Oxo)(μ-carboxylato)diiron(III) Complex with Distinct Iron Sites

A new class of iron proteins with dinuclear iron centers bridged by oxide and carboxylate groups has recently emerged[1] and includes the invertebrate dioxygen carrier hemerythrin,[2] ribonucleotide reductase,[3] purple acid phosphatase,[4] and methane monooxygenase.[5] Prototypical of this class is hemerythrin, which has been shown crystallographically[6] to have a (μ-oxo)bis(μ-carboxylato)diiron core in its met or Fe(III)–Fe(III) form. Five of the six remaining coordination sites are occupied by terminal imidazole ligands from the polypeptide chain, and the sixth site is available for exogenous ligand binding. Thus, methemerythrin has an inherently asymmetric binuclear unit. Spectroscopic studies of ribonucleotide reductases and purple acid phosphatases indicate that the diiron centers in these proteins are also asymmetric.[7,8] Interest in this new class has prompted the synthesis of inorganic complexes with similar structural motifs. Prominent among these analogues are (μ-oxo)bis(μ-carboxylato)diiron(III) complexes with tridentate face-capping ligands such as HB(pz)₃,[9,10] TACN,[11] and other triamines,[12] which model remarkably well the UV–vis,
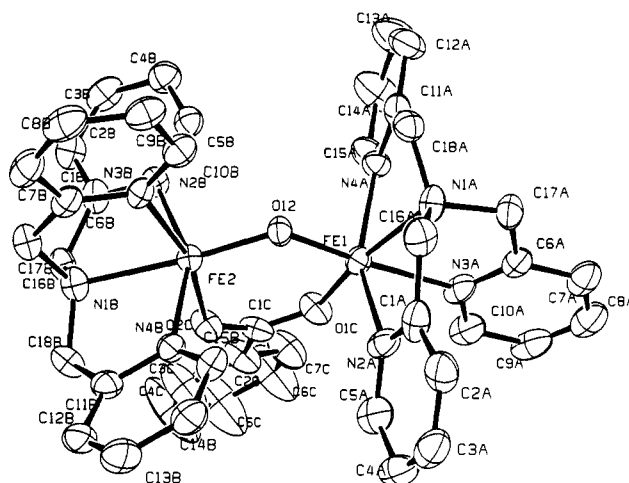

Figure 1. ORTEP representation of [Fe₂(TPA)₂O(OBz)]³⁺ with the thermal ellipsoids drawn at the 50% probability level (hydrogen atoms are omitted for clarity).

NMR, Raman, and magnetic properties of the binuclear iron sites in methemerythrin and ribonucleotide reductase. However, none of these complexes model the asymmetry of protein sites. In our efforts to model the active sites of these iron–oxo proteins, we have discovered a new family of (μ-oxo)(μ-carboxylato)diiron(III) complexes by using tetradentate tripodal ligands. Of these, the complexes derived from tris(2-pyridylmethyl)amine (TPA)[13] assemble in an unsymmetric fashion; their structure and properties are reported here.

Treatment of 2 equiv each of TPA·HClO₄ and triethylamine in methanol with 2 equiv of Fe(ClO₄)₃·xH₂O and 1 equiv of sodium benzoate results in the formation of a greenish brown solid on standing. Elemental analysis affords [Fe₂(TPA)₂O(OBz)]-(ClO₄)₃ (1) as the formula for the complex.[14] Analogous complexes with acetate[15] (2), propionate,[16] and diphenyl phosphate[17] have also been prepared and afford satisfactory elemental analyses.

(1) Que, L., Jr.; Scarrow, R. C. *ACS Symp. Ser.* **1988**, *372*, 152–178. Lippard, S. J. *Angew. Chem., Int. Ed. Engl.* **1988**, *27*, 344–361.
(2) Wilkins, P. C.; Wilkins, R. G. *Coord. Chem. Rev.* **1987**, *79*, 195–214. Klotz, I. M.; Kurtz, D. M., Jr. *Acc. Chem. Res.* **1984**, *17*, 16–22. Sanders-Loehr, J.; Loehr, T. M. *Adv. Inorg. Biochem.* **1979**, *1*, 235–252.
(3) Reichard, P.; Ehrenberg, A. *Science (Washington, D.C.)* **1983**, *221*, 514–519.
(4) Anatanaitis, B. C.; Aisen, P. *Adv. Inorg. Biochem.* **1983**, *5*, 111–136.
(5) Fox, B. G.; Sererus, K. K.; Münck, E.; Lipscomb, J. D. *J. Biol. Chem.* **1988**, *22*, 10553–10556. Ericson, A.; Hedman, B.; Hodgson, K. O.; Green, J.; Dalton, H.; Bentsen, J. G.; Beer, R. H.; Lippard, S. J. *J. Am. Chem. Soc.* **1988**, *10*, 2330–2332. Prince, R. C.; George, N. G.; Saras, J. C.; Cramer, S. P.; Patel, R. N. *Biochim. Biophys. Acta* **1988**, *952*, 220–228.
(6) Stenkamp, R. E.; Sieker, L. C.; Jensen, L. H. *J. Am. Chem. Soc.* **1984**, *106*, 618–622. Sheriff, S.; Hendrickson, W. A.; Smith, J. L. *J. Mol. Biol.* **1987**, *197*, 273–296.
(7) Atkin, C. L.; Thelander, L.; Reichard, P.; Lang, G. *J. Biol. Chem.* **1973**, *248*, 7464–7472.
(8) Antanaitis, B. C.; Aisen, P.; Lilienthal, H. R. *J. Biol. Chem.* **1983**, *258*, 3166–3172.
(9) Abbreviations used: OBz, benzoate; OAc, acetate; OPr, propionate; HB(pz)₃, hydrotris(pyrazolyl)borate; TACN, 1,4,7-triazacyclononane; TPA, tris(2-pyridylmethyl)amine; Me₃TACN, 1,4,7-trimethyl-1,4,7-triazacyclononane; tpbn, *N,N,N',N'*-tetrakis(2-pyridylmethyl)-1,4-butanediamine; bpy, 2,2'-bipyridine; N₅, *N,N,N'*-tris(2-benzimidazolyl-methyl)-*N'*-(2-hydroxyethyl)-1,2-ethanediamine; N₃, bis(2-benz-imidazolylmethyl)amine; HDP, (*o*-hydroxybenzyl)bis(2-pyridyl-methyl)amine; HPTA, *N,N'*-(2-hydroxy-1,3-propylene)bis(*N*-(carbox-ymethyl)glycine).
(10) Armstrong, W. H.; Spool, A.; Papaefthymiou, G. C.; Frankel, R. B.; Lippard, S. J. *J. Am. Chem. Soc.* **1984**, *106*, 3653–3667.
(11) Wieghardt, K.; Pohl, K.; Gebert, W. *Angew. Chem., Int. Ed. Engl.* **1983**, *22*, 727. Hartman, J. R.; Rardin, R. L.; Chaudhuri, P.; Pohl, K.; Wieghardt, K.; Nuber, B.; Weiss, J.; Papaefthymiou, G. C.; Frankel, R. B.; Lippard, S. J. *J. Am. Chem. Soc.* **1987**, *109*, 7387–7396.

(12) Toftlund, H.; Murray, K. S.; Zwack, P. R.; Taylor, L. F.; Anderson, O. P. *J. Chem. Soc., Chem. Commun.* **1986**, 191–193. Gomez-Romero, P.; Casan-Pastor, N.; Ben-Hussein, A.; Jameson, G. B. *J. Am. Chem. Soc.* **1988**, *110*, 1988–1990.
(13) Anderegg, G.; Wenk, F. *Helv. Chim. Acta* **1967**, *50*, 2330–2332.
(14) Anal. Calcd for [Fe₂(TPA)₂O(OBz)](ClO₄)₃, C₄₃H₄₁Cl₃Fe₂N₈O₁₅: C, 45.78; H, 3.64; N, 9.94; Cl, 9.45. Found: C, 45.75; H, 3.83; N, 9.71; Cl, 9.19.
(15) Anal. Calcd for [Fe₂(TPA)₂O(OAc)](ClO₄)₃·2H₂O, C₃₈H₄₃Cl₃Fe₂N₈O₁₇: C, 41.42; H, 3.93; N, 10.17; Cl, 9.65. Found: C, 41.32; H, 3.93, N, 9.84; Cl, 9.81.
(16) Anal. Calcd for [Fe₂(TPA)₂O(OPr)](ClO₄)₃, C₃₉H₄₁Cl₃Fe₂N₈O₁₅: C, 41.30; H, 4.15; N, 9.88. Found: C, 41.35; H, 3.99; N, 9.93.
(17) Anal. Calcd for [Fe₂(TPA)₂O{O₂P(OPh)₂}](ClO₄)₃·2CH₃COCH₃, C₅₄H₅₈Cl₃Fe₂N₈O₁₉P: C, 47.27; H, 4.26; N, 8.17; P, 2.26; Cl, 7.75. Found: C, 46.98; H, 4.61; N, 8.49; P, 2.19; Cl, 7.67.

Table I. Structural and Spectroscopic Parameters of (μ-Oxo)diiron(III) Complexes

	$[Fe_2(TPA)_2O(OBz)]^{3+}$	$[Fe_2(TPA)_2O(OAc)]^{3+}$	$[(HB(pz)_3Fe)_2O(OAc)_2]^a$	$[Fe_2O(OAc)_2Cl_2(bpy)_2]^b$
$r_{Fe-O(oxo)}$, Å	1.804 (5)	1.800 (4)	1.780 (2)	1.783 (4)
	1.776 (4)	1.790 (5)	1.788 (2)	1.787 (4)
$r_{Fe-O(carbox)}$, Å	1.984 (5)	1.972 (6)	2.040 (2)	2.144 (4)
	2.046 (5)	2.038 (6)	2.041 (2)	2.009 (4)
			2.050 (3)	2.011 (6)
			2.040 (2)	2.156 (4)
$r_{Fe-amine}$, Å	2.190 (6)	2.198 (7)		
	2.218 (6)	2.242 (6)		
r_{Fe-N}, Å	2.115 (6)	2.125 (6)	2.153 (3)	2.146 (5)
	2.132 (7)	2.128 (6)	2.159 (3)	
	2.185 (6)	2.199 (7)	2.200 (3)	2.204 (5)
	2.131 (6)	2.133 (6)	2.150 (3)	2.155 (5)
	2.138 (6)	2.154 (6)	2.148 (3)	
	2.118 (6)	2.105 (6)	2.176 (3)	2.212 (5)
r_{Fe-Fe}, Å	3.241 (1)	3.243 (1)	3.1457 (6)	3.151 (1)
∠Fe–O–Fe, deg	129.7 (3)	129.2 (2)	123.6 (1)	123.9 (2)
δ, mm/s^c	0.45	0.45	0.52	0.37
ΔE_Q, mm/s^c	1.52	1.45	1.60	1.80
$-2J$, cm^{-1}	238 (234)^d		244	264
g_0	2.04 (2.0)^d		2.00	1.90
TIP, 10^{-5} emu/mol	0.0 (2.2)^d		2.2	80
% impurity ($S = {}^5/_2$)	0.06 (0.04)^d		0.02	1.0

^{a} From ref 10. ^{b} From ref 27. ^{c} At 4.2 K, relative to iron metal at room temperature. ^{d} Fit with g_0 fixed at 2.0.

Caution! Perchlorate salts are potentially explosive and should be handled with extreme care.

Single-crystal X-ray diffraction analysis of 1′ [18] and 2′ [19] reveals a (μ-oxo)(μ-carboxylato)diiron(III) core with the tripodal ligand occupying the remaining coordination sites on each iron (Figure 1). Other examples of such doubly bridged cores can be found in the complexes $[Fe_2(HDP)_2O(OBz)]BPh_4$ [20] and $Na_6[Fe_2(HPTA)O(CO_3)]_2$. [21] Relevant iron bond lengths for 1′ and 2′ are compared in Table I. The oxo bridge gives rise to short Fe–O bonds (average 1.793 Å), while the carboxylate bridge restricts the Fe–Fe separation to 3.24 Å and the Fe–O–Fe angle to 129°. These metrical parameters are similar to those found for the binuclear sites of several of the iron–oxo proteins[1] and emphasizes the point that such doubly bridged binuclear complexes cannot be excluded as possible structures for the metal centers in ribonucleotide reductase and purple acid phosphatase, which have yet to be characterized crystallographically. Indeed, the Fe–Fe separations of the doubly bridged complexes approach those found in methemerythrin[6] and ribonucleotide reductase[22] more closely than those of the triply bridged complexes.[10-12]

The structures of 1′ and 2′ have further interesting features. The coordination environments of the two iron atoms in the complex are different. The oxo bridge is trans to the tertiary amine nitrogen on Fe2 and cis to the tertiary amine nitrogen on Fe1. The pyridine that is trans to the oxo bridge on Fe1 is characterized by a longer Fe–N bond relative to the remaining five Fe–N_{py} bonds in the complex. Such trans effects have been observed for other oxo-bridged complexes.[8,10] In addition, the carboxylate is also unsymmetrically bridged due to the differing trans ligands on Fe1 and Fe2. It is not clear why the complexes have chosen to adopt
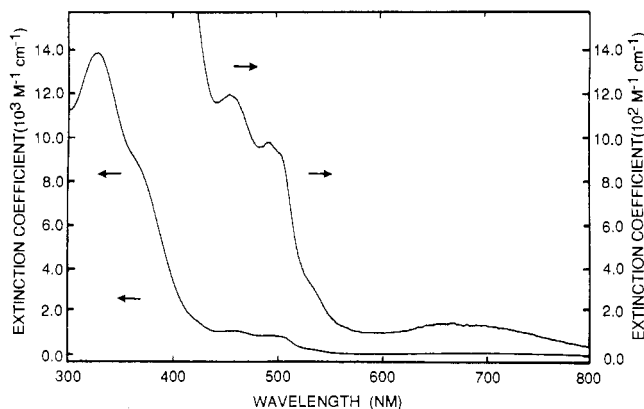

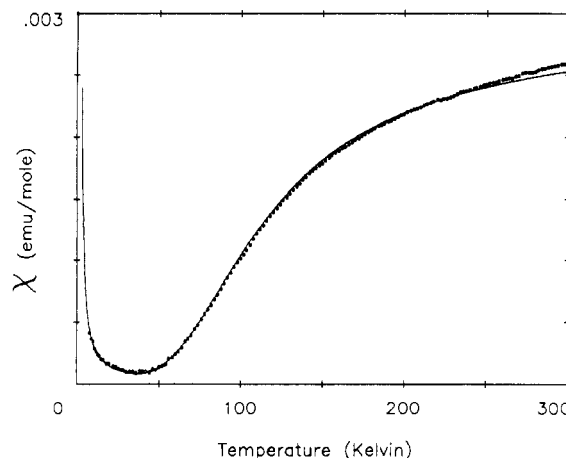**Figure 2.** Electronic spectrum of $[Fe_2(TPA)_2O(OBz)]^{3+}$ in acetonitrile.

Figure 3. Magnetic susceptibility of $[Fe_2(TPA)_2O(OBz)](ClO_4)_3$ plotted as a function of temperature. The solid line corresponds to the theoretical fit to the data (dots).

this mode of coordination, but this mode is observed for both crystallographically characterized complexes. These structures appear to be maintained in solution on the basis of their NMR spectra. In contrast, the structure of the related complex $[Fe_2(HDP)_2O(OBz)]BPh_4$,[20] where one of the pyridines on each tripod ligand has been replaced by a phenolate, has a pseudo-2-fold rotation axis, and the oxo bridge is trans to both tertiary amine nitrogens. The TPA complexes thus represent the first binuclear

(18) Diffraction-quality crystals were obtained by allowing the methanolic reaction mixture to stand in an EtOAc bath. $[Fe_2(TPA)_2O(OBz)](ClO_4)_3 \cdot 2H_2O$ crystallized in the monoclinic space group $P2_1/n$ with a = 11.669 (15) Å, b = 19.568 (20) Å, c = 22.285 (12) Å, and β = 102.24 (8)°. The structure was determined at −84 °C from 5445 out of a total of 8854 reflections with R = 0.064 and R_w = 0.080. Complete details of the structure will be published elsewhere.

(19) $[Fe_2(TPA)_2O(OAc)](ClO_4)_3 \cdot H_2O$-solvate crystallized in the monoclinic space group $P2_1/n$ with a = 20.774 (46) Å, b = 22.312 (5) Å, c = 10.372 (7) Å, and β = 104.14 (12)°. The structure was determined at −88 °C from 6324 out of a total of 9147 reflections with R = 0.078 and R_w = 0.091. Complete details will be published elsewhere.

(20) Yan, S.; Que, L., Jr.; Taylor, L. F.; Anderson, O. P. *J. Am. Chem. Soc.* **1988**, *110*, 5222–5224.

(21) Jameson, D. L.; Xie, C.-L.; Hendrickson, D. N.; Potenza, J. A.; Schugar, H. J. *J. Am. Chem. Soc.* **1987**, *109*, 740–746.

(22) Scarrow, R. C.; Maroney, M. J.; Palmer, S. M.; Que, L., Jr.; Salowe, S. P.; Stubbe, J. *J. Am. Chem. Soc.* **1986**, *108*, 6832–6834.

iron complexes with oxo and carboxylate bridges having distinct iron sites. The only other unsymmetric complex is $[N_5FeOFeCl_3]^+$, a singly bridged diiron complex with a six-coordinate and a four-coordinate metal center.[23] However, neither of these complexes adequately mimic the asymmetry found in methemerythrin and its anion complexes.

The UV–vis spectrum of **1** (Figure 2) exhibits absorption features with maxima near 330, 400, 490, and 650 nm. These have also been observed for methemerythrin,[24] ribonucleotide reductase,[25] and the synthetic (μ-oxo)bis(μ-carboxylato)diiron(III) complexes,[10] but their precise nature is not yet understood. That these spectral features are found for oxo-bridged diiron(III) complexes with either one or two bridging carboxylates suggests that they are associated with the presence of the bent oxo bridge and that the carboxylates do not directly contribute to the spectral features.

The number of carboxylate bridges does not appear to affect the magnetic properties of these oxo- and carboxylato-bridged complexes (Table I). SQUID magnetic susceptibility data on **1** from 4 to 200 K are shown in Figure 3 and can be fit with the standard Boltzmann distribution equation for an antiferromagnetically coupled diferric complex.[26] With g fixed at a value of 2.0, the fit yielded $2J = -234$ cm^{-1} ($\mathcal{H} = -2JS_1 \cdot S_2$), TIP = 2.2 $\times 10^{-5}$ emu/mol, and 0.04% high-spin ferric impurity ($F = 4.00$).[27] An improved fit can be obtained with the following parameters: $g = 2.04$, $2J = -238$ cm^{-1}, TIP = 0, and 0.06% high-spin ferric impurity ($F = 2.89$, Figure 3). The J value for **1** compares favorably with those found for other (μ-oxo)bis(μ-carboxylato)-diiron(III) complexes,[10,11,12,28] and this similarity emphasizes the fact that the strength of the antiferromagnetic coupling interaction is determined almost solely by the oxo bridge.

A third property that characterizes the presence of the oxo bridge is the large quadrupole splitting observed in the Mössbauer spectrum of the complex. **1** and **2** exhibit quadrupole doublets with ΔE_Q values of ca. 1.5 mm/s, comparable to those observed for other synthetic complexes (Table I). The doublets are somewhat broadened ($\Gamma = 0.32$ mm/s), probably reflecting the differences in the iron sites. It is clear, however, that these structural differences do not translate into large differences in the quadrupole splittings. The challenge thus remains for synthetic inorganic chemists to design molecules that mimic the large differences in ΔE_Q values as found in ribonucleotide reductase[7] and the purple acid phosphatases.[29,30]

In summary, we have synthesized a new family of (μ-oxo)(μ-carboxylato)diiron(III) complexes using tetradentate tripodal ligands such as TPA and HDP,[20] which have structural, spectroscopic, and magnetic properties comparable to those of the (μ-oxo)bis(μ-carboxylato)diiron complexes. The similarities emphasize the point that both (μ-oxo)diiron(III) units with one or two carboxylate bridges are suitable candidates for the active sites of enzymes such as ribonucleotide reductase and purple acid phosphatase, which as yet have not been crystallographically characterized.

(31) (a) Visiting scientist from Nankai University, Tianjin, People's Republic of China. (b) Gray Freshwater Biological Institute, University of Minnesota.

Department of Chemistry   **Shiping Yan**[31a]
University of Minnesota   **David D. Cox**
Minneapolis, Minnesota 55455   **Linda L. Pearce**
    Carlos Juarez-Garcia[31b]
    Lawrence Que, Jr.*

Department of Chemistry   **Jian H. Zhang**
University of New Orleans   **Charles J. O'Connor**
New Orleans, Louisiana 70122

Excited States of Polyoxometalates as Oxidatively Resistant Initiators of Hydrocarbon Autoxidation. Selective Production of Hydroperoxides

Some of the largest scale industrial processes such as autoxidation of the hydrocarbons, cyclohexane, and *p*-xylene (eq 1) as well as a myriad of small scale halogenation and other reactions carried out in industrial and academic laboratories are radical-chain processes.[1,2] For alkanes, these processes are generally not

$$\underset{\substack{\text{hydrocarbon}\\\text{substrate}}}{RH} + O_2 \xrightarrow{\text{initiator}} \underset{\text{alcohol}}{ROH} + \underset{\text{ketone}}{R=O} +$$

many other products (1)
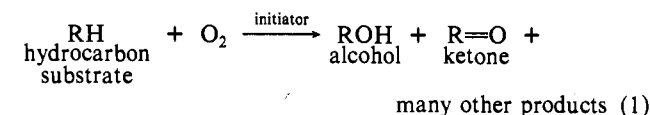
very selective and nearly all depend on initiators to start and sustain reaction. Alkane autoxidation reactions are as messy as they are important. The autoxidation of cyclohexane in conjunction with the Du Pont nylon process produces over 120 products![2] Both the thermal and photochemical conditions used for autoxidation initiation generally do not permit selective production of the useful hydroperoxides, ROOH, the usual initial nonradical kinetic products in alkane reactions (eq 2). Indeed, the hydroperoxides

$$RH + O_2 \rightarrow ROOH \qquad (2)$$

themselves readily initiate chains under typical thermal and photochemical free-radical reaction conditions.[1] In massive and miniscule scale reactions alike, the initiators in the above reactions are consumed. In context with our goal of developing thermodynamically stable yet experimentally tractable catalysts for the selective functionalization of alkanes and other kinetically difficult transformations,[3] we report here a polyoxometalate-based system that efficiently initiates hydrocarbon autoxidation with unusually

(23) Romero, P. G.; DeFotis, G. C.; Jameson, G. B. *J. Am. Chem. Soc.* **1986,** *108,* 851–853.

(24) Garbett, K.; Darnell, D. W.; Klotz, I. M.; Williams, R. J. P. *Arch. Biochem. Biophys.* **1969,** *135,* 419–434.

(25) Peterson, L.; Gräslund, A.; Ehrenberg, A.; Sjöberg, B.-M.; Reichard, P. *J. Biol. Chem.* **1980,** *255,* 6706–6712.

(26) O'Connor, C. J. *Prog. Inorg. Chem.* **1982,** *29,* 203–283.

(27) $F = 10^5[\sum(\chi_{calc} - \chi_{obs})^2/n]^{1/2}$.

(28) Vincent, J. B.; Huffman, J. C.; Christou, G.; Li, Q.; Nanny, M. A.; Hendrickson, D. N.; Fong, R.; Fish, R. H. *J. Am. Chem. Soc.* **1988,** *110,* 6898–6900.

(29) Averill, B. A.; Davis, J. C.; Burman, S.; Zirino, T.; Sanders-Loehr, J.; Loehr, T. M.; Sage, J. T.; Debrunner, P. G. *J. Am. Chem. Soc.* **1987,** *109,* 3760–3767.

(30) Debrunner, P. G.; Hendrich, M. P.; de Jersey, J.; Keough, D. T.; Sage, J. T.; Zerner, B. *Biochim. Biophys. Acta* **1983,** *745,* 103–106.

(1) (a) Sheldon, R. A.; Kochi, J. K. *Metal-Catalyzed Oxidations of Organic Compounds;* Academic Press: New York, 1981; Chapter 2. (b) Parshall, G. W. *Homogeneous Catalysis. The Applications and Chemistry of Catalysis by Soluble Transition Metal Complexes;* Wiley-Interscience: New York, 1980; Chapter 10. (c) Weissermel, K.; Arpe, H.-J. *Industrial Organic Chemistry;* Verlag Chemie: New York, 1978; p 212.

(2) Tolman, C. A.; Druliner, J. D.; Nappa, M. J.; Herron, N. In *Activation and Functionalization of Alkanes;* Hill, C. L., Ed.; Wiley: New York, 1989; Chapter 10.

(3) (a) Hill, C. L.; Brown, R. B. *J. Am. Chem. Soc.* **1986,** *108,* 536. (b) Faraj, M.; Hill, C. L. *J. Chem. Soc., Chem. Commun.* **1987,** 1487. (c) Brown, R. B.; Renneke, R.; Hill, C. L. *Prepr. Am. Chem. Soc., Div. Pet. Chem.* **1987,** *32*(1), 205. (d) Hill, C. L.; Renneke, R. F.; Faraj, M. K.; Brown, R. B., Jr. *The Role of Oxygen in Chemistry and Biology;* Ando, W., Ed.; Elsevier: New York, 1988; p 185. (e) Renneke, R. F.; Hill, C. L. *J. Am. Chem. Soc.* **1988,** *110,* 5461. (f) Faraj, M.; Lin, C.-H.; Hill, C. L. *New J. Chem.* **1988,** *12,* 745. See references cited in each.